

# Islanding Detection for Inverter-Based Distributed Generation Using Support Vector Machine Method

Biljana Matic-Cuka, *Student Member, IEEE*, and Mladen Kezunovic, *Fellow, IEEE*

**Abstract**—In this paper, a new islanding detection method for single phase inverter-based distributed generation is presented. In the first stage of the proposed method, a parametric technique called autoregressive signal modeling is utilized to extract signal features from voltage and current signals at the point of common coupling with the grid. In the second stage, advanced machine learning technique based on support vector machine, which takes calculated features as inputs is utilized to predict islanding state. The extensive study is performed on the IEEE 13 bus system and feature vectors corresponding to various islanding and non-islanding conditions are used for support vector machine classifier training and testing. Simulation results show that the proposed method can accurately detect system islanding operation mode 50 ms after the event starts. Further, the robustness of the proposed method is analyzed by examining its performances in the systems with multiple distributed generations, and when system loading condition, grid disturbance types, and characteristics are altered.

**Index Terms**—Autoregressive (AR) signal modeling, inverter-based distributed generation (DG), islanding detection, smart grid, support vector machine (SVM).

## I. INTRODUCTION

THE RISE in the energy demand, environmental concerns and favorable government policies introduced new directions and challenges in the power grid development. The conventional grid is the network with a few large, centralized generation sources at the transmission system that supplies passive users at distribution system. This is drifting away toward the network with many renewable distributed generation (DG) sources at all voltage levels. In the last decade due to significant development in the power electronics and digital control technology, a number of large scale, offshore and onshore wind generation units and farms have been installed in the transmission system. The photovoltaic (PV) systems began to evolve recently when the cost of power electronic inverters decreased and PVs found broad applications at the distribution level as small residential units. The power inverter is the most important element of the PV system and it acts as the

Manuscript received July 11, 2013; revised December 15, 2013, April 3, 2014, and June 2, 2014; accepted July 4, 2014. Date of publication August 7, 2014; date of current version October 17, 2014. This work was supported by the U.S. Department of Energy Office of Electricity Delivery and Energy Reliability under Project “The Future Grid to Enable Sustainable Energy Systems” conducted through National Science Foundation Industry (NSF I)/University Cooperative Research Program (UCRC) Power Systems Engineering Research Center (PSerc). Paper no. TSG-00483-2013.

The authors are with the Department of Electrical and Computer Engineering, Texas A&M University, College Station, TX 77843-3128 USA (e-mail: bmatic@tamu.edu; kezunov@ece.tamu.edu).

Color versions of one or more of the figures in this paper are available online at <http://ieeexplore.ieee.org>.

Digital Object Identifier 10.1109/TSG.2014.2338736

interface between the PV and the grid. The main function of the power inverter is to convert direct current (dc) power generated at PV cells to alternating current (ac) power and obtain synchronization with the grid. Depending on the size of the PV system, power inverters could have single phase or three phase structure [1]. The PV systems used in the roof top residential units have single phase topology while large size PV systems used in power plants have three phase topology.

Despite the fact that renewable DG brings many economic and environmental benefits it introduces new challenges in power system control, operation, and protection. One of the most important impacts of the DG integration in the distribution system is unintentional islanding. Islanding occurs when DG continues to energize a portion of the system while being disconnected from the main grid. Since the island is unregulated, its behavior is unpredictable and voltage, frequency and other power quality parameters may have unacceptable limits. The out-of-phase reclosing is possible and high transient inrush currents may damage local devices. Also unintentional islanding in the system may create electric shock if energized conductors that are assumed to be disconnected are touched by public or utility workers. Thus, the islanded systems should be de-energized promptly. According to the IEEE Std. 1547 [2] DG shall detect the islanding for any possible islanding conditions and cease to energize the area within 2 s for small voltage and frequency signal variation. A large voltage changes below 0.88 pu or above 1.2 pu and for the frequency variations more than 60.5 Hz or less than 59.3 Hz at the point of common coupling (PCC) islanding should be detected within 0.16 s.

In this paper, new anti-islanding method for single phase inverter-based DG that uses support vector machine (SVM) classifier is presented. The paper is organized as follows. In Section II the status of the current research of the islanding detection topic is presented. The theoretical background of the autoregressive (AR) signal modeling and SVM are described in Section III. In Section IV SVM based islanding detection method is proposed. The following Section V provides system modeling details, events simulation procedures and pattern generation approach. The effect of the data window size on the classifier performance is analyzed too. The implementation details are described in Section VI. The conclusions are summarized in Section VII. At the end of the paper an elaborate list of relevant references is given.

## II. BACKGROUND

The islanding occurs when a section of the power system is accidentally disconnected from the main grid while being

energized by the local DG. Since, islanded system operates without utility supervision; the values of the power system parameters, such as voltage and frequency are unpredictable. Their new operating points satisfy balances of active and reactive power between the DG and the local load, which determines severity of the islanding condition. In the case of large active and/or reactive power mismatch voltage and frequency magnitudes will change significantly immediately after the disconnection, which may cause a safety hazard, hence the DG has to be disconnected quickly through an anti-islanding scheme. For smaller power mismatches, the system parameters will rise or decrease slowly before setting to the new operating point.

In the past, many anti-islanding methods have been proposed and these methods can be characterized as communication based or local measurement based methods. For the large scale DG integration, such as bulk wind plant integration, communication based methods known as transfer trip, are used. However, for the small DG units in the distribution system those methods are impractical due to cost of installation. Hence local measurement based passive and active methods are used instead. These methods rely only on the system parameters measured at PCC and both have their own advantages and disadvantages. The performance of the anti-islanding method is often defined by nondetection zone (NDZ) concept. The NDZ represents the mismatch in active and reactive power generated by DG and dissipated by the local load for which the method will not be able to differentiate between islanding and normal operation [3].

The active methods are embedded into a control circuit of the power inverter and they are designed to inject small disturbances into the DG output. In the case of islanding those disturbances will cause system parameters to rise above the acceptable limits, trigger protective relays, and disconnect the system at the PCC. The active frequency drift (AFD) [4], improved AFD [5], sandia frequency shift (SFS) [6], fuzzy SFS [7], automatic phase shift (APS) [8], sliding mode frequency shift (SMFS) [9], impedance measurement [10], singular and dual harmonic current injections [11], [12], high frequency signal injection [13] output power variations [14], reactive power variation and control control [15], [16] are examples of the active methods. The active methods are categorized by small NDZ but they may deteriorate power quality during normal power system operation [17]. Besides, active methods may mis-operate in the system with multiple DGs due to mutual interference and cancelation of the injected disturbances [18] or they may have an effect on the system stability [19].

On the other hand, the passive methods discriminate islanding from normal condition based on the measurements of system parameters at the PCC. The signal parameter measurements or some features extracted from them are compared to the predefined thresholds. The most common methods of this type are under/over voltage, under/over frequency [17], rate of change of frequency [20], phase jump detection [21], rate of change of frequency with power [22], rate of change of power with total harmonic distortion (THD) [23], voltage unbalance and total harmonic distortion of current signal [24],

voltage and power factor change [25], energy mismatch for the harmonics [26] etc. These methods do not have any negative impact on the grid operation, but they are characterized by larger NDZ than active methods. To decrease NDZ of the passive methods advanced signal processing tools such as Duffing oscillations [27] wavelet transform [28], [29], S-Transform [29] have been utilized. However, these methods may be characterized by higher computational complexity and sensitivity to the noise. The biggest challenge in designing the passive anti-islanding method to select the most important parameter(s) and to set the right threshold low enough to detect islanding for small power generation/load mismatch and high enough to not operate for external events, such as system components switching or system faults still remains.

Recently, it was recognized that learning from data is a useful way to analyze power system disturbances and in some cases it may be the most accurate method to extract the information and characterize some power system events [30]. The work in [31] proposes islanding detection for inverter based DG using a Bayesian classifier and achieves high accuracy. However, due to high computational burden of running ESPRIT constantly on the new data windows this scheme assumes knowledge of the islanding event's start time to initiate ESPRIT run and confirm islanding occurrence. Thus, this method is impractical for the implementations in the real systems. Reference [32] uses a decision tree approach and it shows great robustness for the external grid events while it has 83.33% accuracy for islanding detection. The work in [33] applies adaptive boosting (AdaBoost) technique to improve decision tree accuracy. However, this approach is sensitive to outliers and the noisy data due to nature of the AdaBoost processing [34]. The decision tree classifier is utilized again in [35] and robust and reliable method is presented. The method has a few drawbacks. First, the training data set used in the study has highly unbalanced class distribution. This phenomenon is well known in the machine learning theory and leads to overly optimistic results toward majority class [36]. Also, the signal sampling rate of 40 kHz used in the study is much higher than the typical 2–5 kHz sampling rate of the digital relays and recorders. The work in [37] uses a fuzzy role approach to detect islanding state and its performance shows great sensitivity to presence of the noise in the data set, and is dependent on the threshold setting on the decision tree split criterion. Reference [38] proposes method that uses a fuzzy expert system approach and requires complex calculation to obtain input parameters of the classifier.

SVM tool has become a popular tool for power systems analysis, such as load or device type identification in an electrical system [39], [40], power system transient stability assessment [41], distance relay blocking and blackout mitigation [42]. SVM is studied in [43] for the islanding detection. This paper uses wavelet transform (WT) to extract features from the current signal at PCC. However, it is well known that the major drawback for the WT is its sensitivity to the noisy conditions. Thus, based on the literature review there is a lack of an islanding method that is fast, reliable, easy to implement and has low computational burden.

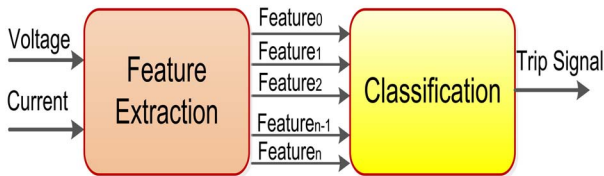


Fig. 1. Diagram of the proposed islanding detection technique.

In this paper, new anti-islanding method for single phase inverter-based DG is presented. This method uses SVM classifier to predict whether the system operates in the islanded mode. A parametric method called the AR modeling is used to extract signal features from voltage and current measurements at PCC and these coefficients are used as inputs to the SVM classifier. The method is tested on the IEEE-13 [44] bus system which is modeled in PSCAD/EMTDC, while MATLAB and LIBSVM [45] packages are used to extract features from the signals and to train and test the SVM models. To analyze accuracy and robustness of the proposed method a number of islanding and nonislanding events, such as DG, load, capacitor or motor switching and external faults under different loading conditions and DG participations are simulated.

### III. THEORETICAL BASIS

The proposed method is based on the principle that variations in the power spectral density (PSD) functions of the voltage and current signals at PCC may be used to determine whether the DG system operates in an islanded mode. It is well known that when connected to the grid inverter-based DGs produce harmonics due to high-frequency switching, dead time and dc link voltage ripple. These harmonics are maintained by the filters and inverter embedded control solutions and should be kept below 5% according to IEEE Std. 1547. The magnitude of the harmonics depends heavily on the grid impedance value and will increase in the islanded mode of operation. This also happens in the case of the grid transients caused by faults or system component switching. Thus, the PSD function of the voltage and current signals maybe used as a valid index in the islanding detection.

In this paper, voltage and current signals are measured with instrument transformers at PCC and their instantaneous values are processed to extract AR coefficients. These features are fed into the SVM models generated offline and islanding state is predicted. In the case of islanding the trip signal is sent to the circuit breaker at PCC to disconnect DG from the grid. The diagram of the proposed anti-islanding scheme is shown in Fig. 1. In this section the theory behind techniques used in the feature extraction and classification steps is presented.

#### A. Autoregressive Modeling

A spectral analysis, defined as a problem of assessing how the power of the signal is being distributed over the frequency, has found many applications in the power system monitoring, protection and operation. The most commonly used methods for spectral analysis are nonparametric, such as fast fourier transform (FFT) and discrete wavelet transform (DWT). However, FFT is characterized by poor spectral

estimation, so called low frequency resolution which depends on the length of the signal being processed. On the other hand, DWT has high frequency resolution, but it has a few major drawbacks. DWT performance depends on the right selection of the mother wavelet and decomposition level. Moreover, DWT is characterized by an inability to obtain correct signal features in noisy conditions and it requires additional preprocessing to suppress signal noise. This will increase algorithm complexity and time delay.

As opposed to nonparametric methods that do not require any prior knowledge about the signal, in the case of model-based methods one may assume that the signals are generated from certain models. The AR parametric modeling has found broad applications in analysis of biomedical signals [46] and recently has been discovered as a powerful tool for power system disturbances analysis, such as low frequency oscillations estimation [47] and fault detection and location [48]. In this paper, AR is used as feature extraction tool for the islanding detection problem.

This section describes the basic theory for parametric modeling of signals using AR method. By using AR approach the signal is represented as the response of a linear time invariant system with white noise as input, where the system is modeled by finite number of poles. In a  $AR(p)$  model, the data sample at time  $t$  is defined by the following equation:

$$x(t) = - \sum_{i=1}^p a_i x(t-i) + b_0 e(t) \quad (1)$$

where

- $a_i$  AR coefficients;
- $e(t)$  white Gaussian noise;
- $b_0$  noise variance.

This is equivalent to  $x(t)$  being the output of an all-pole system  $H(z)$  whose input is the white noise  $e(t)$ . The transfer function of the all-pole system is

$$H_{AR}(z) = \frac{b_0}{1 + \sum_{i=1}^p a_i z^{-i}} \quad (2)$$

As a result, estimating the frequency spectrum of  $x(t)$  becomes estimating the model parameters  $a_i$  under a selected criterion. The covariance expression of the AR process may be used to estimate  $a_i$ ,  $i = 1 \dots p$  parameters by replacing the true auto-covariance function  $r(k) = E\{x(t)x(t-k)\}$  with estimates obtained from data [49] (see the Appendix)

$$r(k) + \sum_{i=1}^p a_i r(k-i) = 0, \quad k \geq 0 \quad (3)$$

and

$$r(0) + \sum_{i=1}^p a_i r(-i) = b_0^2, \quad k = 0. \quad (4)$$

From (3) and (4) for  $k = 1, \dots, p$  Yule-Walker or normal equations are obtained

$$\begin{bmatrix} r(0) & r(-1) & \dots & r(-p) \\ r(1) & r(0) & \dots & r(1-p) \\ & & \dots & \\ & & & \dots \\ r(p) & r(p-1) & \dots & r(0) \end{bmatrix} \begin{bmatrix} 1 \\ a_1 \\ \cdot \\ \cdot \\ a_p \end{bmatrix} = \begin{bmatrix} b_0^2 \\ 0 \\ \cdot \\ \cdot \\ 0 \end{bmatrix}. \quad (5)$$

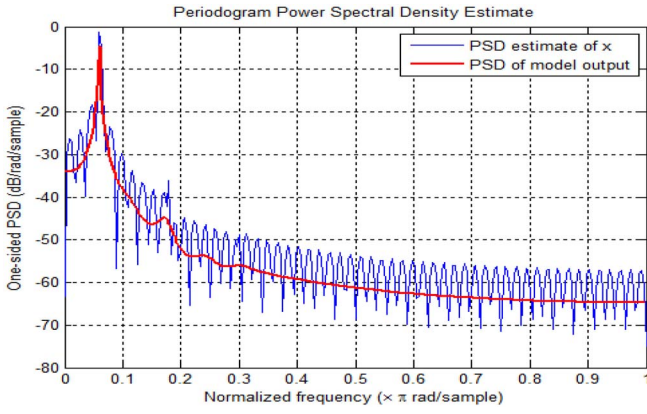


Fig. 2. Periodogram versus AR PSD estimation of the voltage signal at PCC for the 0% active and reactive power mismatch.

If  $r\{(k)\}_{k=0}^p$  were known we could solve (5) for

$$\theta = [a_1, \dots, a_p]^T \quad (6)$$

by using all but the first row. Once  $\theta$  is obtained,  $b_0^2$  can be found easily from (4). We can write the equation for the order  $p$  as follows:

$$R_{p+1} \begin{bmatrix} 1 \\ \theta_p \end{bmatrix} = \begin{bmatrix} b_0^2 \\ 0 \end{bmatrix}. \quad (7)$$

In order to reduce the number of flops to calculate  $\{\theta_p, b_0^2\}$  the order recursive solution called Levinson-Durbin algorithm [49] is used.

The AR model gives inherent data compression without loss of essential information and smooth frequency spectrum can be obtained from AR coefficients, while maintaining all important signal features. Fig. 2 aligns PSD functions obtained using FFT and AR of the voltage signal at the PCC for the 0% active and reactive power mismatch. The zero power mismatches represents system state when RLC load parameters are tuned to the certain values that the active/reactive power dissipated by the load is equal to the active/reactive power generated by the inverter. Thus, there is no power infeed from the grid side to the load node.

Figs. 3–5 show AR coefficients of voltage and current signals for the islanding and nonislanding events. The difference between coefficients for islanding and nonislanding events is apparent. This makes AR processing proper feature extraction tool and further validates good classification results.

### B. Support Vector Machine Classifier

SVM has been developed by Vapnik [50] and is becoming a popular machine learning tool due to great ability to generalize performances. Its principle is based on the structural risk minimization (SRM) that minimizes an upper bound on the expected risk, opposed to the error on the training data used by neural network (NN). While NN performance is dependent on the size of the training data set and has a number of parameters that should be tuned, SVM may make good prediction using smaller data sets and has fewer parameters to be adjusted [30].

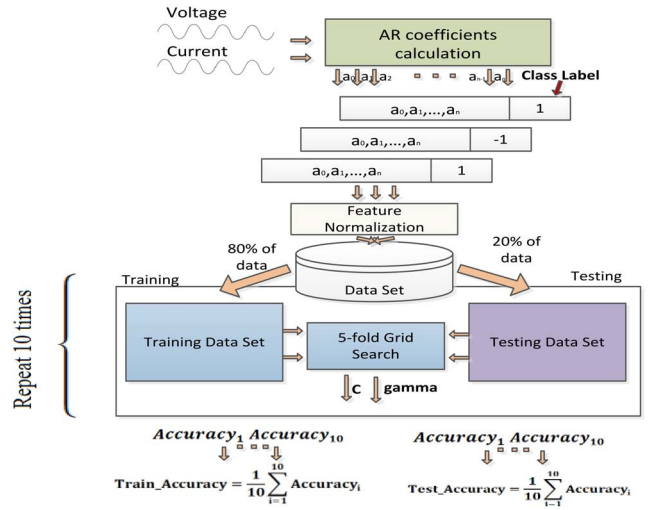


Fig. 3. Anti-islanding scheme design and validation.

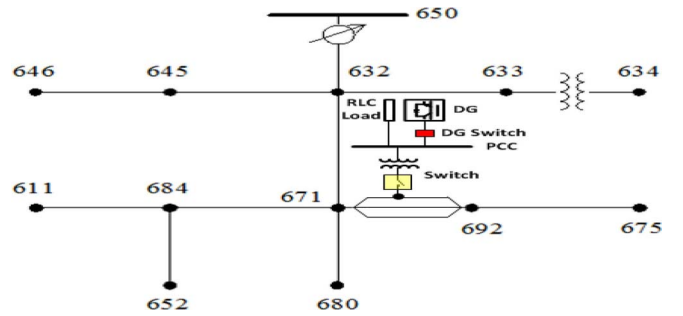


Fig. 4. Diagram of the IEEE 13 distribution test system [44].

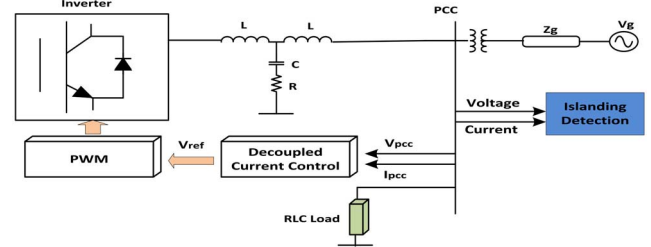


Fig. 5. DG system used in the study.

The data vectors used to train classifier consist of the feature vectors and one class label. The aim of the SVM classifier is to produce data model in the training phase that will predict the class label in the testing phase where only feature attributes are used as inputs [51]. A special characteristic in designing a SVM is that, instead of the dimension reduction commonly employed in conventional pattern recognition systems, the input space in a SVM is nonlinearly mapped onto a high-dimensional feature space. The result is that the classes are more likely to be linearly separable than in a low-dimensional feature space. A SVM classifier uses a kernel function  $K(x_i, x_j)$  that relates a subset of the training vectors, called support vectors  $x_i$ , to the testing data vectors  $x_j$  to nonlinearly project the input space onto a high-dimensional feature space.

Given a training set of instances and class label pairs  $(x_i, y_i)$   $i = 1 \dots l$ , where  $x_i \in R^n$  and  $y_i \in \{1, -1\}^l$ , the SVM requires the solution of the following optimization problem [51]:

$$\min_{w,b,\xi} \frac{1}{2} |w|^2 + C \left( \sum_{i=1}^l \xi_i \right) \quad (8)$$

subject to

$$y_i (w^T \phi(x_i) + b) \geq 1 - \xi_i, \quad (\forall i) \quad \xi_i \geq 0. \quad (9)$$

Here training vectors  $x_i$  are mapped into a higher dimensional space by the function  $\phi$ . In the training process the support vectors from the training data will be selected and used to predict unseen data. Parameter  $C > 0$  is the penalty factor of the error term and may be seen as factor that controls the tradeoff between separation margin and training errors, while  $\|w\|$  is a norm to the vector perpendicular to the separation hyperline and  $\xi_i$  are slack variables which measure degree of misclassification [50].

Furthermore,  $K(x_i, x_j) = \phi(x_i)^T \phi(x_j)$  represents the kernel function. Despite many kernels being proposed by researchers, in this paper radial bias function (RBF)

$$K(x_i, x_j) = e^{-\gamma \|x_i - x_j\|^2}, \quad \gamma > 0 \quad (10)$$

kernel is used.  $C$  and  $\gamma$  can be determined experimentally through a grid search and cross-validation process. To estimate the best values of the  $C$  and  $\gamma$  parameters the values of both parameters are varied in increments of the power of 2. For the any parameter combination a  $k$ -fold cross-validation is applied. First, the training data set is divided into  $k$  subsets of equal size. The SVM classifier is then trained  $k$  times and in the  $l$ th iteration,  $l = 1, 2, \dots, k$ , the classifier is trained using all subsets except the  $l$ th subset. The trained classifier is then tested using only the  $l$ th subset, and the classification error for this subset is calculated. In such a way, each training subset is tested once and the cross-validation accuracy is the percentage of the data which are correctly classified. Finally the average of these errors is taken as the expected prediction error. This procedure is repeated for the available  $C$  and  $\gamma$  parameter values and the best pair that gives the highest estimation accuracy is selected.

#### IV. PROPOSED SOLUTION

The steps in designing and validation of the proposed SVM-based anti-islanding protection scheme are presented in Fig. 3. The instantaneous values of voltage and current signals are obtained in multiple PSCAD/EMTDC simulations afterwards they are processed using Yule-Walker method to calculate AR coefficients and noise variance. The signal window of 50 ms and model order  $p = 30$  are used for the AR coefficients calculations. The model order is selected using common rule that AR order should be around one third of the data window size. The voltage and current signals are decomposed into 31 parameters (30 AR coefficients and noise variance) each. Thus, for every simulation run, 62 feature parameters (31 parameters of the current and 31 parameters of the voltage current signals) and a class label that describes operation mode

of the system (“1” for islanding and “-1” for nonislanding) are stored as a single database entry.

To assure that each feature in a feature vector is unbiased and properly scaled feature normalization is applied

$$\hat{x}_i = \frac{x_i - \mu_i}{\sigma_i}, \quad i = 1 \dots k \quad (11)$$

where

- $k$  feature dimension;
- $\sigma_i$  standard deviation of the  $i$ th feature;
- $\mu_i$  mean value of the  $i$ th feature.

To estimate SVM model parameters and to evaluate performance of the selected model on the unseen data set the fivefold cross validation and bootstrap method [52] are used, respectively. The bootstrapping is a general statistics technique that iterates the computation of the algorithm accuracy on a resampled dataset. The Bootstrap iterator will generate a user defined number of independent training and testing data set splits to check whether proposed data model is biased to the training and testing data set. For the SVM classifier used in this paper two parameters have to be selected: the regularization parameter  $C$  and kernel parameter  $\gamma$ . The values of the both parameters  $C$  and  $\gamma$  are varied in the range from  $2^{-5}$  to  $2^{10}$  and  $2^8$  to  $2^{-8}$ , respectively. For the any parameter combination fivefold cross-validation is performed. The data set is split in five parts, where four parts are used to train and one part to test, the parts are rotated so that error is evaluated evenly across all examples. The values  $C = 8$  and  $\gamma = 0.0625$  are shown to be the best combination for the proposed application. This process is repeated for 10 replications, until the error rate converges, with different training and test splits. The average detection accuracy computed in this way is a good estimator of the SVM model generalization accuracy.

#### V. EXAMPLE OF APPLICATION

##### A. Power System Description

In order to demonstrate proposed concept, a study case using IEEE 13-bus test system shown in Fig. 4 [44] is modeled using PSCAD/EMTDC simulation tool. The sampling frequency used in the study is 2 kHz. A 5 kVA single phase 120V DG is connected to A phase of the node 692. The DG is connected to the distribution system through a single phase 0.12/4.16 kV transformer. The structure of the single phase inverter-based DG is presented in Fig. 5. The DG system parameters are listed in Table I. The low-pass filter, with the parameters in Table I is employed as interface between inverter and the grid to reduce the effect of inverter's harmonics. The decoupled current control interface presented in [15] is used in the study. The inverter control is adjusted so that DG operates at unity power factor as recommended by the IEEE Std. 1547. In this arrangement DG does not provide reactive power support while supplying maximum active power to the grid. To investigate effects of the multiple DGs interaction and impact of the second DG switching to the method performance, the inverter-based DG with the same control interface and parameters is added to a phase A of the node 675.

TABLE I  
PARAMETERS OF THE SYSTEM

Parameter	Value
Voltage	120 V
DG Output Power	5k W
Switching Frequency	8k Hz
Input DC Voltage	400 V
Filter Resistance (R)	1 Ω
Filter Inductance (L)	3 mH
Filter Capacitance (C)	12μF

B. Data Set Generation

In order to design and evaluate proposed method, 700 different islanding and nonislanding events are simulated. The following process is used to select optimal data set.

- 1) The arbitrary data set is generated and model parameters and prediction accuracy are estimated.
- 2) Then, additional data points are added to the data set and the parameter tuning and accuracy are then estimated again.
- 3) After several steps of adding additional data to the data set and performing calculation, results for both classifier parameters and accuracy will converge. That means that the optimal data set size is reached.

The data set consists of 700 feature vectors and assigned class labels. The feature vectors represent AR coefficients for voltage and current signals calculated using 50 ms data window captured immediately after transient occurrence. The data set is generated in such a way that the number of islanding (positive) and nonislanding (negative) events is evenly balanced. There are 350 nonislanding and 350 islanding events. Noneven spread of the positive and negative events may lead to biased detection of one category of the events. The set of 350 islanding cases is generated for different combinations of the active and reactive power mismatches. An adjustable RLC load is connected in parallel between the DG inverter and the grid and islanding conditions are simulated by opening the single phase switch (Fig. 5). The mismatch power generated by DG and dissipated by the load is varied up to 40% for active and 5% for reactive power. The set of 350 nonislanding cases is generated by applying faults at different locations in the grid and by switching static loads, motor loads, and capacitor banks at different points in the system as well as switching second DG at node 675. The single, double, and three phase faults whose resistance and duration are varied are simulated. The resistance is changed from 1Ω to 5Ω and duration is set as 2 ms, 4 ms, and permanent faults. The islanding and nonislanding events are simulated for light system loading conditions up to 40% of the base load maintaining the constant load power factor. More details about case generation may be found in Table II.

C. Feature Extraction

The main purpose of this section is to present AR modeling as feature extraction tool. Events presented in this section cause minimal deviation in the system parameters and are

TABLE II  
GENERATED DATA SET

Cases	No. of Data Samples	Description
Islanding	300	±40 % active power and ±5% reactive power mismatch
Non-islanding	25	Load Switching
Non-islanding	25	Capacitor Switching
Non-islanding	25	Motor Load Switching
Non-islanding	225	Faults
Islanding	25	Light load; various power mismatches
Non-islanding	25	Faults at different locations
Islanding	25	While Second DG is connected
Non islanding	25	Second DG Switching

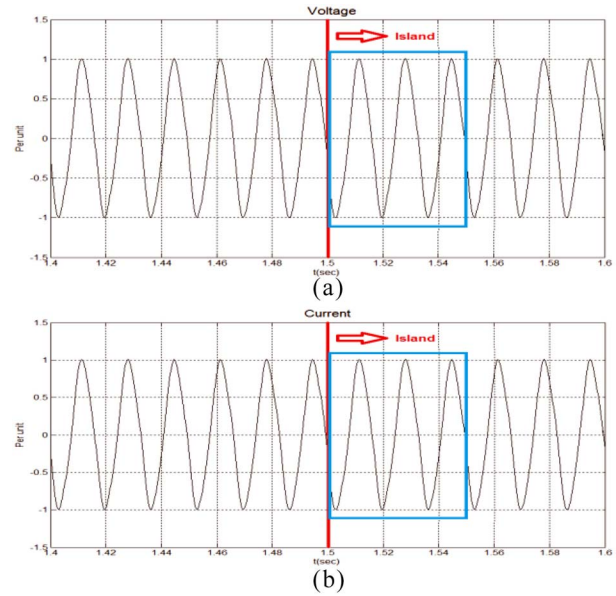


Fig. 6. (a) PCC voltage and (b) PCC current for an islanding event for a zero active/reactive power mismatch.

among the most challenging to classify. Fig. 6 shows the system response of the voltage and current signals at PCC of an islanding event for zero active/reactive power mismatches.

For this event voltage and current magnitudes do no change. Figs. 7–9 show grid fault, capacitor switching and load switching, respectively. For load switching, the magnitude of the voltage increases 3% while for the capacitor switching and grid fault events voltage magnitudes decrease 2% and 5%, respectively.

On the other hand, the current magnitudes change in such a way to maintain constant real power output. The 50 ms data window is used to calculate noise variance AR coefficients for the voltage and current signals. The noise variances are listed in Table III, while AR coefficients are presented in Figs. 10 and 11. AR modeling as feature extraction tool was able to extract unique representations of the signals.

D. Results and Discussion

Because of the random nature of the experiment, slight differences may occur between the performances of SVM models

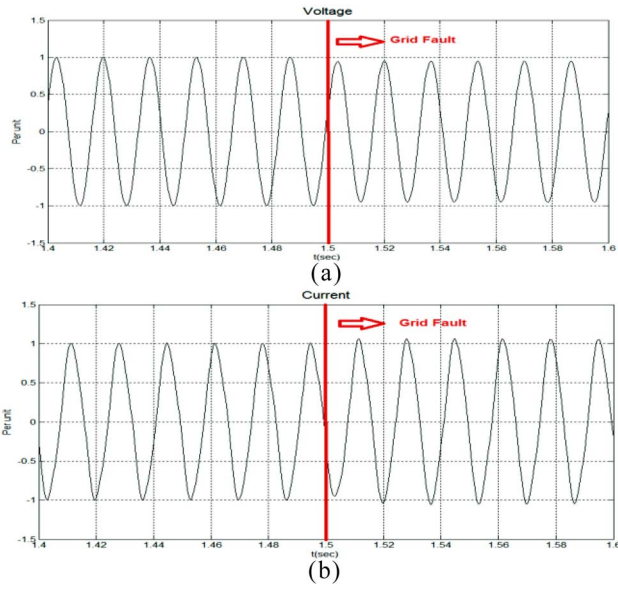


Fig. 7. (a) PCC voltage and (b) PCC current for a-phase grid fault event at bus 675.

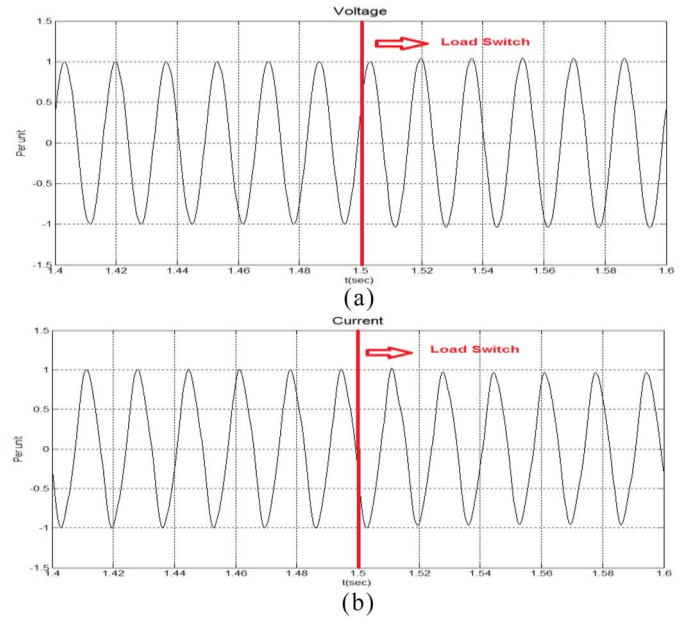


Fig. 9. (a) PCC voltage and (b) PCC current for load switching event at bus 675.

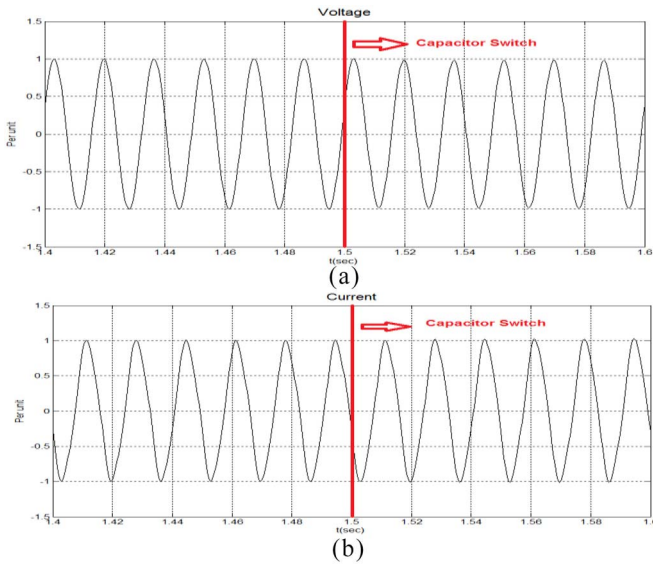


Fig. 8. (a) PCC voltage and (b) PCC current for capacitor switching event at bus 692.

for different training/testing data sets. In order to achieve good generalization performances, the training/testing process was repeated ten times by randomly selecting the training/testing data set from the simulated event database using the above obtained parameters and procedure shown in Fig. 3. The average prediction error is calculated as a sum of obtained errors divided by the number of iterations.

The average error is used to determine generalization error of proposed classifier. The purpose of this step is to evaluate generalization performance of the algorithm on unseen examples.

The overall prediction accuracy for the training data set is estimated to be 100%. Table IV shows classification accuracy for testing data set per event type. In order to analyze

TABLE III  
NOISE VARIANCE

Event	Voltage noise variance	Current noise variance
Islanding	0.0001	0.00001
Grid Fault	0.00002	0.00002
Capacitor Switching	0.0001	0.00001
Load Switching	0.0001	0.00004

performances of the proposed algorithm in detail the test data is separated according to the event type, such as islanding, static load, motor, capacitor and DG switching and fault event. This allows observing how the classifier is performing under each type of the event. The classification error for non-islanding events is 0% and it proves algorithm robustness and insensitivity to the grid faults and switching transients.

The algorithm performances have been tested on the feature vectors that capture transient after its occurrence, the analysis is extended for the feature vectors that contain only part of the transient. The test is performed for the nonislanding events shown in Figs. 7–9. The test starts at transient occurrence and finishes 50 ms after the transient occurrence. The 50 ms window slides through the signals and calculates AR coefficients for each step, then these coefficients are fed into the classifier and predictions are generated. Figs. 12 and 13 show AR coefficients for voltage and current signals for grid fault event shown in Fig. 7. In this test the classifier predictions were not affected by partial transient consideration.

The classification accuracy for islanding conditions is estimated to be 98.94%. Table V summarizes classification accuracy for testing data set. The detail description of the events shown in Tables IV and VI may be found in Table II. The overall accuracy of the proposed algorithm is estimated to be 99.49% with 0.6277% uncertainty. One way of measuring

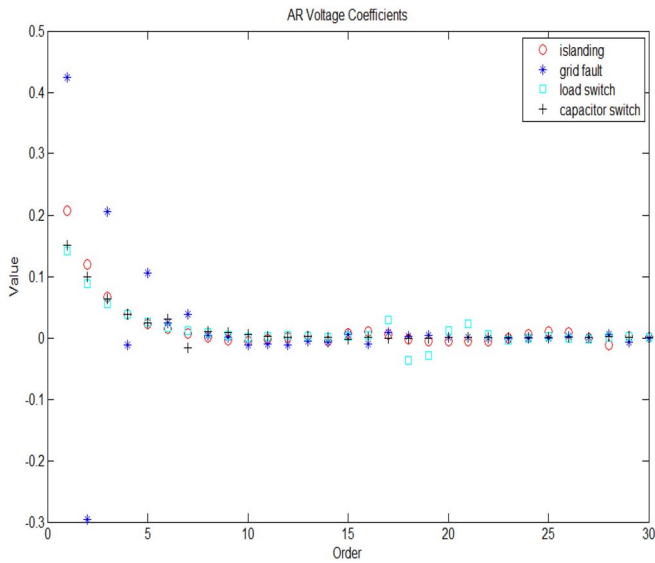


Fig. 10. AR coefficients of the voltage signal at PCC for islanding, fault, load switching and capacitor switching events.

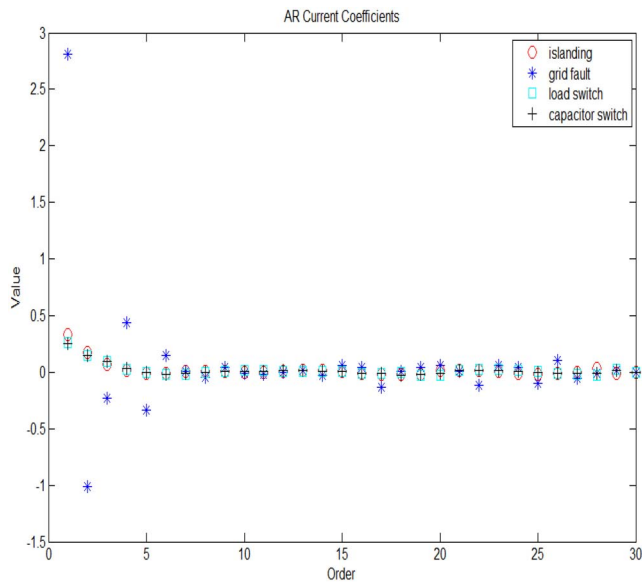


Fig. 11. AR coefficients of the current signal at PCC for islanding, fault, load switching and capacitor switching events.

TABLE IV  
CLASSIFICATION RESULTS FOR EVENT TYPE

Cases	Testing data set prediction accuracy (%)
<b>Fault Event</b>	100
<b>Capacitor Switching</b>	100
<b>Static Load Switching</b>	100
<b>Motor Load Switching</b>	100
<b>Islanding</b>	98.94

uncertainty is to calculate standard deviation of accuracy across replications of the same experiment

$$\sigma = \sqrt{\frac{1}{N} \sum_{i=1}^{10} (A_i - \mu_{\text{accuracy}})^2} \quad (12)$$

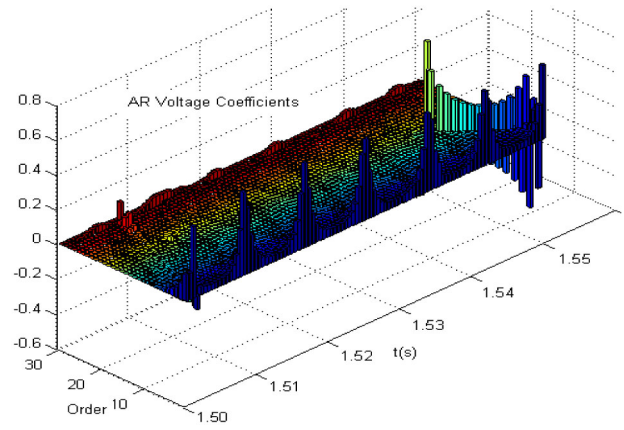


Fig. 12. AR coefficients of the voltage signal at PCC for grid fault event.

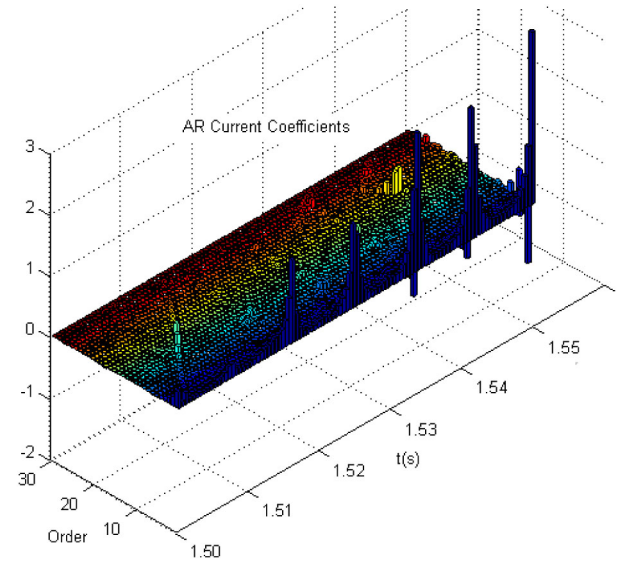


Fig. 13. AR coefficients of the current signal at PCC for grid fault event.

TABLE V  
CLASSIFICATION RESULTS FOR TESTING DATA SET

Cases	Prediction Accuracy on the testing data set (%)
<b>Non-Islanding</b>	100
<b>Islanding</b>	98.94
<b>Total</b>	99.49

TABLE VI  
CLASSIFICATION RESULTS FOR DIFFERENT WINDOW SIZES

Cases	Prediction Accuracy on the testing data set (%)			
	10ms	20ms	30ms	40ms
<b>Fault Event</b>	100	100	100	100
<b>Capacitor Switching</b>	100	100	100	100
<b>Static Load Switching</b>	100	100	100	100
<b>Motor Load Switching</b>	100	100	100	100
<b>Islanding</b>	96.96	96.96	97.12	97.71

where

- $N$  number of repetitions;
- $A_i$  detection accuracy for  $i$ th repetition;
- $\mu_{\text{accuracy}}$  mean of the detection accuracy.

It is evident that prediction accuracy decreases slightly comparing to the training data accuracy and thus it proves good generalization performance of the algorithm. Also, the proposed algorithm shows great robustness in the light loading conditions and impact of the second DG on its operation may be neglected.

The impact of the data window size on performance of the proposed algorithm is analyzed as well. The algorithm is tested for 10, 20, 30, and 40 ms. For these window sizes AR model order  $p = 6, 12, 19$  and  $24$  are used to obtain AR coefficients from voltage and current signals. The same procedure described in Fig. 3 is utilized. As before, the five-fold cross-validation on the training data set using the simple grid search is performed. And the same values of  $C = 8$  and  $\gamma = 0.0625$  are shown to be optimal combination of the parameters. The overall prediction accuracy for the training data set is estimated to be 100%. The results of this investigation for testing data set are presented in Table VI. Again the algorithm shows high robustness in performance for nonislanding events and miss-operation error for external grid events is estimated to be 0 for all cases. As expected the results clearly show that prediction accuracy decrease with reduction in the window length. Still, performances for the smaller windows have decent classification accuracy and may be applicable in the systems where trade between speed and accuracy should be adjusted toward fast islanding detection.

## VI. IMPLEMENTATION DETAILS

The proposed method utilizes 50 ms sliding window to extract feature vectors from voltage and current signals at PCC. These vectors are fed into SVM classifier and predictions are made for each step. In case of the islanding trip signal will be sent to the DG switch (Fig. 4). to disconnect DG from the grid. The proposed method shows great performances for the active power mismatch up to 40% and reactive power mismatch up to 5% while it may fail to detect islanding for the larger mismatches and therefore it is assumed that this method operates in parallel with Over/Under Voltage (OUV) and Over/Under Frequency (OUF) relays at the PCC. These relays should be set to detect islanding for more than 40% of active and 5% of reactive power mismatches which is high enough to avoid misoperations due to external nonislanding events. OUV and OUF relays trip fast and accurate in the case of islanding for large power mismatches.

Also, it is important to mention that detection time delay of the proposed method does not depend on the real/reactive power mismatch because the same number of AR parameters, as well as SVM support vectors, is utilized for any event, independently of the real/reactive power mismatch. The detection time delay may be defined as the sum of the time delay caused by AR calculation, which is directly related to the length of the data window, and the number of the SVM support vectors, which is related to the size of the training data set. Therefore, after the training phase, in deployment the delay may be considered constant. Beside this, the time delay is affected by the speed of the processor.

## VII. CONCLUSION

This paper has explored an approach to detect islanding using support vector machine and the following conclusions have been reached.

- 1) Autoregressive coefficients of voltage and current signals at point of common coupling have been used as input feature vectors for support vector machine classifier.
- 2) The proposed method is insensitive to external grid disturbances, such as grid faults and component switching and does not have any negative effect on the power quality of the grid.
- 3) The results indicate that this method can detect islanding with a high degree of accuracy.
- 4) The proposed method is fast and detection time delay does not depend on the real/reactive power mismatch.

## APPENDIX

In this section, covariance from (3) is derived [49]. First, we multiply (1) with  $x^*(t-k)$  and taking expectation yields to

$$r(k) + \sum_{i=1}^p a_i r(k-i) = b_0 E\{e(t)x^*(t-k)\}, \quad k > 0. \quad (13)$$

We can write transfer function as

$$H(z) = \frac{B(z)}{A(z)} = \sum_{k=0}^{\infty} h_k z^{-k}, \quad h_0 = 1. \quad (14)$$

It gives

$$y(t) = H(z)e(t) = \sum_{k=0}^{\infty} h_k e(t-k) \quad (15)$$

$$\begin{aligned} E\{e(t)x^*(t-k)\} &= E\left\{e(t) \sum_{s=0}^{\infty} h_s^* e^*(t-k-s)\right\} \\ &= \sigma^2 h_{-k}^*. \end{aligned} \quad (16)$$

For

$$h_k = 0, \quad k < 0 \quad r(k) + \sum_{i=1}^p a_i r(k-i) = b_0 \sigma^2 h_{-k}^* \quad (17)$$

since

$$h_s = 0 \text{ for } s < 0 \quad r(k) + \sum_{i=1}^p a_i r(k-i) = 0, \quad k \geq 0. \quad (18)$$

## ACKNOWLEDGMENT

The authors would like to thank Dr. V. Malbasa for his valuable comments throughout the work reported in this paper.

## REFERENCES

- [1] R. Teodorescu *et al.*, *Grid Converters for Photovoltaic and Wind Power Systems*. Hoboken, NJ, USA: Wiley, 2011.
- [2] *IEEE Standard for Interconnecting Distributed Resources With Electric Power Systems*, IEEE Standard 1547-2003, 2003.
- [3] L. A. C. Lopes and H. Sun, "Performance assessment of active frequency drifting islanding detection methods," *IEEE Trans. Energy Convers.*, vol. 21, no. 1, pp. 171–180, May 2006.

- [4] G. A. Kern, "SunSine300: Utility interactive AC module anti-islanding test results," in *Proc. 26th IEEE Photovolt. Spec. Conf.*, Anaheim, CA, USA, 1997, pp. 1265–1268.
- [5] A. Yafaoui, B. Wu, and S. Kouro, "Improved active frequency drift anti-islanding detection method for grid connected photovoltaic systems," *IEEE Trans. Power Electron.*, vol. 27, no. 5, pp. 2367–2375, May 2012.
- [6] M. E. Ropp *et al.*, "Determining the relative effectiveness of islanding detection methods using phase criteria and non detection zones," *IEEE Trans. Energy Convers.*, vol. 15, no. 3, pp. 290–296, Sep. 2000.
- [7] H. Vahedi and M. Karrari, "Adaptive fuzzy sandia frequency-shift method for islanding protection of inverter-based distributed generation," *IEEE Trans. Power Del.*, vol. 28, no. 1, pp. 84–92, Jan. 2013.
- [8] G. Hung, C. Chang, and C. Chen, "Automatic phase-shift method for islanding detection of grid-connected photovoltaic inverter," *IEEE Trans. Energy Convers.*, vol. 18, no. 1, pp. 169–173, Mar. 2003.
- [9] S. Yuyuma *et al.*, "A high speed frequency shift method as a protection for islanding phenomena of utility interactive PV systems," *Sol. Energy Mater. Sol. Cells*, vol. 35, nos. 1–4, pp. 477–486, 1994.
- [10] M. C. Wrinch, "Negative sequence impedance measurement for distributed generator islanding detection," Ph.D. dissertation, Dept. Elect. Comput. Eng., Univ. British Columbia, Vancouver, BC, Canada, 2008.
- [11] G. Hernandez-Gonzalez and R. Iravani, "Current injection for active islanding detection of electronically-interfaced distributed resources," *IEEE Trans. Power Del.*, vol. 21, no. 3, pp. 1698–1705, Jul. 2006.
- [12] W. Cai, B. Liu, S. Duan, and C. Zou, "An islanding detection method based on dual-frequency harmonic current injection under grid impedance unbalanced condition," *IEEE Trans. Ind. Informat.*, vol. 9, no. 2, pp. 1178–1187, May 2013.
- [13] D. D. Reigosa, F. Briz, C. B. Charro, P. Garcia, and J. M. Guerrero, "Active islanding detection using high-frequency signal injection," *IEEE Trans. Ind. Appl.*, vol. 48, no. 5, pp. 1588–1597, Sep./Oct. 2012.
- [14] C. Jeraputra and P. N. Enjeti, "Development of a robust anti-islanding algorithm for utility interconnection of distributed fuel cell powered generation," *IEEE Trans. Power Electron.*, vol. 19, no. 5, pp. 1163–1170, Sep. 2004.
- [15] J. Zhang *et al.*, "An improved islanding detection method for a grid-connected inverter with intermittent bilateral reactive power variation," *IEEE Trans. Power Electron.*, vol. 28, no. 1, pp. 268–278, Jan. 2013.
- [16] Y. Zhu *et al.*, "A novel RPV (reactive-power-variation) antiislanding method based on adapted reactive power perturbation," *IEEE Trans. Power Electron.*, vol. 28, no. 11, pp. 4998–5012, Nov. 2013.
- [17] W. I. Bower and M. Ropp, "Evaluation of islanding detection methods for utility-interactive inverters in photovoltaic systems," Sandia Nat. Labs., Albuquerque, NM, USA; Sandia Nat. Labs., Livermore, CA, USA, Rep. SAND2002-3591, 2002.
- [18] L. A. C. Lopes and Y. Zhang, "Islanding detection assessment of multi-inverter systems with active frequency drifting methods," *IEEE Trans. Power Del.*, vol. 23, no. 1, pp. 480–486, Jan. 2008.
- [19] X. Wang, W. Freitas, V. Dinavahi, and W. Xu, "Investigation of positive feedback anti-islanding control for multiple inverter-based distributed generators," *IEEE Trans. Power Syst.*, vol. 24, no. 2, pp. 785–795, May 2009.
- [20] A. Samui and S. R. Samantaray, "Assessment of ROCPAD relay for islanding detection in distributed generation," *IEEE Trans. Smart Grid*, vol. 2, no. 2, pp. 391–398, Jun. 2011.
- [21] J. Stevens, R. Bonn, J. Ginn, S. Gonzalez, and G. Kern, "Development and testing of an approach to anti-islanding in utility-interconnected photovoltaic systems," Sandia Nat. Lab., Albuquerque, NM, USA, Tech. Rep. SAND2000-1939, Aug. 2000.
- [22] H. Shyh-Jiler and P. Fu-Sheng, "A new approach to islanding detection of dispersed generators with self-commutated static power converters," *IEEE Trans. Power Del.*, vol. 15, no. 2, pp. 500–507, Apr. 2000.
- [23] A. Danandeh, H. Seyedi, and E. Babaei, "Islanding detection using combined algorithm based on rate of change of reactive power and current THD techniques," in *Proc. 2012 Asia-Pacific Power Energy Eng. Conf. (APPEEC)*, Shanghai, China, pp. 1–4.
- [24] S.-I. Jang and K.-H. Kim, "An islanding detection method for distributed generations using voltage unbalance and total harmonic distortion of current," *IEEE Trans. Power Del.*, vol. 19, no. 2, pp. 745–752, Apr. 2004.
- [25] S. K. Salman, D. J. King, and G. Weller, "New loss of mains detection algorithm for embedded generation using rate of change of voltage and changes in power factors," in *Proc. 7th Int. Conf. Develop. Power Syst. Protect.*, 2001, pp. 82–85.
- [26] M. Liserre, A. Pigazo, A. Dell'Aquila, and V. M. Moreno, "An anti-islanding method for single-phase inverters based on a grid voltage sensorless control," *IEEE Trans. Ind. Electron.*, vol. 53, no. 5, pp. 1418–1426, Oct. 2006.
- [27] H. Vahedi, G. B. Gharehpetian, and M. Karrari, "Application of duffing oscillators for passive islanding detection of inverter-based distributed generation units," *IEEE Trans. Power Del.*, vol. 27, no. 4, pp. 1973–1983, Oct. 2012.
- [28] C. T. Hsieh, J. M. Lin, and S.-J. Huang, "Enhancement of islanding-detection of distributed generation systems via wavelet transform-based approaches," *Int. J. Elect. Power Energy Syst.*, vol. 30, no. 10, pp. 575–580, 2008.
- [29] A. Samui and S. R. Samantaray, "Wavelet singular entropy-based islanding detection in distributed generation," *IEEE Trans. Power Del.*, vol. 28, no. 1, pp. 411–418, Jan. 2013.
- [30] M. H. Bollen and I. Gu, *Signal Processing of Power Quality Disturbances*. Hoboken, NJ, USA: Wiley, Aug. 2006.
- [31] W. K. A. Najj, H. H. Zeineldin, A. H. K. Alaboudy, and W. L. Woon, "A Bayesian passive islanding detection method for inverter-based distributed generation using ESPRIT," *IEEE Trans. Power Del.*, vol. 26, no. 4, pp. 2687–2696, Oct. 2011.
- [32] K. El-Arroudi, G. Joos, I. Kamwa, and D. T. McGillis, "Intelligent-based approach to islanding detection in distributed generation," *IEEE Trans. Power Del.*, vol. 22, no. 2, pp. 828–835, Apr. 2007.
- [33] S. S. Madani, A. Abbaspour, M. Beiraghi, P. Z. Dehkordi, and A. M. Ranjbar, "Islanding detection for PV and DFIG using decision tree and AdaBoost algorithm," in *Proc. 2012 3rd IEEE PES Int. Conf. Exhibit. Innov. Smart Grid Technol. (ISGT Eur.)*, pp. 1–8.
- [34] T. Dietterich, "An experimental comparison of three methods for constructing ensembles of decision trees: Bagging, boosting and randomization," *Mach. Learn.*, vol. 40, no. 2, pp. 139–158, 2000.
- [35] N. W. A. Lidula and A. D. Rajapakse, "A pattern-recognition approach for detecting power islands using transient signals—Part II: Performance evaluation," *IEEE Trans. Power Del.*, vol. 27, no. 3, pp. 1071–1080, Jul. 2012.
- [36] D. A. Cieslak and N. V. Chawla, "Learning decision trees for unbalanced data," in *Machine Learning and Knowledge Discovery in Databases*. Berlin, Germany: Springer, Sep. 2008, pp. 241–256.
- [37] S. R. Samantaray, K. El-Arroudi, G. Joos, and I. Kamwa, "A fuzzy rule-based approach for islanding detection in distributed generation," *IEEE Trans. Power Del.*, vol. 25, no. 3, pp. 1427–1433, Jul. 2010.
- [38] M. Padhee, P. K. Dash, K. R. Krishnanand, and P. K. Rout, "A fast Gauss-Newton algorithm for islanding detection in distributed generation," *IEEE Trans. Smart Grid*, vol. 3, no. 3, pp. 1181–1191, Sep. 2012.
- [39] L. Du *et al.*, "Support vector machine based methods for non-intrusive identification of miscellaneous electric loads," in *Proc. 38th Annu. Conf. IEEE Ind. Electron. Soc.*, Montreal, QC, Canada, Oct. 2012, pp. 4866–4871.
- [40] D. Srinivasan, W. S. Ng, and A. C. Liew, "Neural-network-based signature recognition for harmonic source identification," *IEEE Trans. Power Del.*, vol. 21, no. 1, pp. 398–405, Jan. 2006.
- [41] F. R. Gomez, A. D. Rajapakse, U. D. Annakkage, and I. T. Fernando, "Support vector machine-based algorithm for post-fault transient stability status prediction using synchronized measurements," *IEEE Trans. Power Syst.*, vol. 26, no. 3, pp. 1474–1483, Aug. 2011.
- [42] K. Seethalekshmi, S. N. Singh, and S. C. Srivastava, "A classification approach using support vector machines to prevent distance relay maloperation under power swing and voltage instability," *IEEE Trans. Power Del.*, vol. 27, no. 3, pp. 1124–1133, Jul. 2012.
- [43] N. W. A. Lidula, N. Perera, and A. D. Rajapakse, "Investigation of a fast islanding detection methodology using transient signals," in *Proc. IEEE Power Energy Soc. Gen. Meeting (PES)*, Calgary, AB, Canada, Jul. 2009, pp. 1–6.
- [44] W. H. Kersting, "Radial distribution test feeders," *IEEE Trans. Power Syst.*, vol. 6, no. 3, pp. 975–985, Aug. 1991.
- [45] (2012, Aug.). *LIBSVM from Chih-Wei Hsu and Chih-Jen Lin* [Online]. Available: <http://www.csie.ntu.edu.tw/~cjlin/libsvm/>
- [46] M. Kiyimikb, M. Akinc, and A. Alkanb, "AR spectral analysis of EEG signals by using maximum likelihood estimation," *Comput. Biol. Med.*, vol. 31, no. 6, pp. 441–450, 2001.
- [47] R. W. Wies, J. W. Pierre, and D. J. Trudnowski, "Use of ARMA block processing for estimating stationary low-frequency electromechanical modes of power systems," *IEEE Trans. Power Syst.*, vol. 18, no. 1, pp. 167–173, Feb. 2003.

- [48] S. Thanagasundram, S. Spurgeon, and F. Schlindwein, "A fault detection tool using analysis from an autoregressive model pole trajectory," *J. Sound Vibration*, vol. 317, nos. 3–5, pp. 975–993, Nov. 2008.
- [49] P. Stoica and R. L. Moses, *Spectral Analysis of the Signals*. Upper Saddle River, NJ, USA: Prentice Hall, Apr. 2005.
- [50] V. Vapnik, *The Nature of Statistical Learning Theory* (Information Science and Statistics). New York, NY, USA: Springer, Dec. 1999.
- [51] C. Cortes and V. Vapnik, "Support-vector networks," *Mach. Learn.*, vol. 20, no. 3, pp. 273–297, 1995.
- [52] E. Bradley and R. J. Tibshirani, *An Introduction to the Bootstrap* (Monographs on Statistics and Applied Probability). New York, NY, USA: Chapman & Hall, May 1994.



**Biljana Matic-Cuka** (S'07) received the Master's degree in electrical and computer engineering from the University of Novi Sad, Novi Sad, Serbia, in 2006. She is currently pursuing the Ph.D. degree from the Department of Electrical and Computer Engineering, Texas A&M University, College Station, TX, USA.

Her current research interests include grid integration of renewable energy systems, power system monitoring and protection, signal processing and machine learning applications in power systems, smart grids, and substation automation.



**Mladen Kezunovic** (S'77–M'80–SM'85–F'99) received the Dipl.Ing., M.S., and Ph.D. degrees in electrical engineering in 1974, 1977, and 1980, respectively.

He is currently the Eugene E. Webb Professor with the Department of Electrical and Computer Engineering, Texas A&M University, College Station, TX, USA; the Director of the Smart Grid Center; Site Director of NSF I/UCRC "Power Engineering Research Center, PSec;" and the Deputy Director of another NSF I/UCRC "Electrical Vehicles-Transportation and Electricity Convergence, EV-TEC." His current research interests include digital simulators and simulation methods for relay testing, as well as application of intelligent methods to power system monitoring, control, and protection. He has published over 450 papers; given over 100 seminars, invited lectures and short courses; and consulted for over 50 companies worldwide. He is the Principal of XpertPower Associates, College Station, a consulting firm specializing in power systems data analytics.

Dr. Kezunovic is a Fellow of the IEEE Distinguished Speakers, a member of Conseil International des Grands Réseaux Électriques (CIGRE), and is Registered Professional Engineer in Texas.